Lawrence Berkeley National Laboratory
Recent Work

Title

RECENT RESULTS ON THE NEW PARTICLE STATES BELOW 3.7 GeV PPODUCED IN eV ANNIHILATIONS

Permalink

https://escholarship.org/uc/item/4wc5j4nw

Author

Goldhaber, G.

Publication Date

1976-05-01

00004502704

LBL-4884
c.1

RECENT RESULTS ON THE NEW PARTICLE STATES BELOW 3.7 GeV PRODUCED IN e^+e^- ANNIHILATIONS
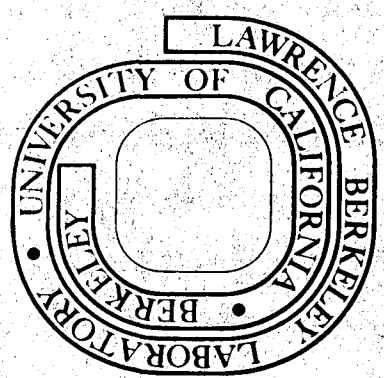
G. Goldhaber

RECEIVED

May 1976

LBL-4884
c.1

DISCLAIMER

00υ04502705

RECENT RESULTS ON THE NEW PARTICLE STATES BELOW 3.7 GeV
PRODUCED IN e^+e^- ANNIHILATIONS[*]

G. Goldhaber[**]

Department of Physics and Lawrence Berkeley Laboratory
University of California, Berkeley, California 94720

The results presented in this talk come from the SLAC-LBL magnetic detector experiment at SPEAR. The new features which give rise to what is "recent" in these results are the following:

(i) Additional running at SPEAR in the Fall of 1975 and Winter of 1976 has increased the integrated luminosity at the ψ/J and ψ' each by about a factor of three. The total hadron sample studied here is approximately 150,000 events at the ψ and 350,000 events at the ψ'.

(ii) The new running was carried out with a "relaxed trigger requirement." This allowed triggering on lower momentum particles.[1]

(iii) By improved geometrical corrections and the application of bubble-chamber kinematical fitting programs, a higher mass resolution of the X states, intermediate between the ψ and ψ', was obtained.

(iv) The magnetic detector was used as a γ-ray pair spectrometer. By inclusion of the proportional chambers in track reconstruction, the measurements allowed the reconstruction of lower electron or positron momenta than possible in earlier work.


Outline

I will discuss the following topics in this talk:

A. Intermediate states between the ψ and ψ' observed via their hadronic decay modes.[2] We have observed three intermediate states, X(3415), X(3500), and X(3550). For X(3415), which is the most prominent, the following decay channels were observed[3]: $4\pi^{\pm}$, $2\pi^{\pm}2K^{\pm}$, $6\pi^{\pm}$, $2\pi^{\pm}$ or $2K^{\pm}$, and $2\pi^{\pm}p\bar{p}$.

B. From an inclusive study of $e^{+}e^{-}$ pairs due to converted γ rays (and Dalitz pairs), the process $\psi' \rightarrow \gamma + X(3415)$ was observed.[4]

C. By further demanding a ψ in the final state with $\psi \rightarrow e^{+}e^{-}$ or $\mu^{+}\mu^{-}$ we have studied the reaction $\psi' \rightarrow \gamma\gamma\psi$. While in our earlier work[5] only the P_{c} was observed,[6] we now find evidence for three distinct states at: 3455 MeV, 3505 MeV, and 3545 MeV. The first of these does not show any signal above background in the hadronic decay modes studied. The last two can be associated with the X's mentioned above. Taken altogether, we thus have evidence[4] for four distinct intermediate states between the ψ and ψ'.

D. We have made a search for the reaction

$$\psi \rightarrow \gamma X$$
$$\quad\quad |_{\rightarrow\ p\bar{p}}$$
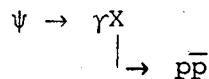
with $M(p\bar{p})$ near 2800 MeV. Evidence for such a state was presented by the DASP group from DESY at the 1975 Photon Conference at SLAC. We find no clear signal for this reaction and present upper limits for it.[7]

A. Intermediate States Between the ψ and ψ'
Observed Via Their Hadronic Decay Modes

Following our original observation of the X states,[2] we have now studied a much larger sample of ψ' decays. In this study corrections for some small residual geometrical distortions were made. The data we report here has also been fitted by the kinematical fitting program, SQUAW, to the hypotheses:

$$\psi' \to \gamma + \pi^+\pi^-\pi^+\pi^- \quad , \tag{1}$$

$$\psi' \to \gamma + \pi^+\pi^-K^+K^- \quad , \tag{2}$$

and
$$\psi' \to \gamma + 3\pi^+\ 3\pi^- \quad . \tag{3}$$

Figure 1 shows the missing mass squared distribution for reaction (1). As may be noted, a peak in missing mass squared (MM^2) consistent with gamma

$$\psi'(3684) \to \pi^+\pi^+\pi^-\pi^- X \quad \text{Preliminary}$$

XBL 764-1623
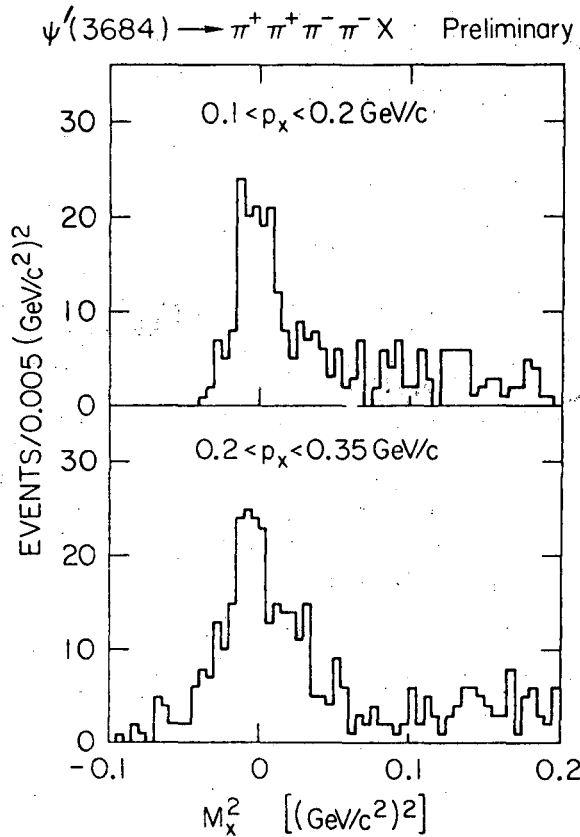
Fig. 1. The missing mass squared distribution in $\psi' \to 4\pi^\pm + X$ for two missing momentum intervals as shown.

production is observed. A cut was made to select $|MM^2| < 0.05$ GeV/c. As we have shown earlier, a major decay mode of the ψ' is the cascade process:

$$\psi' \to \pi^+\pi^- + \psi \quad . \tag{4}$$

The missing mass against all combinations of the $\pi^+\pi^-$ systems is shown in Fig. 2a for four-prong events and in Fig. 2b for five- and six-prong events. To avoid the decay channel (4) in the study of the X final states, we make a

MISSING MASS AGAINST $\pi^+\pi^-$
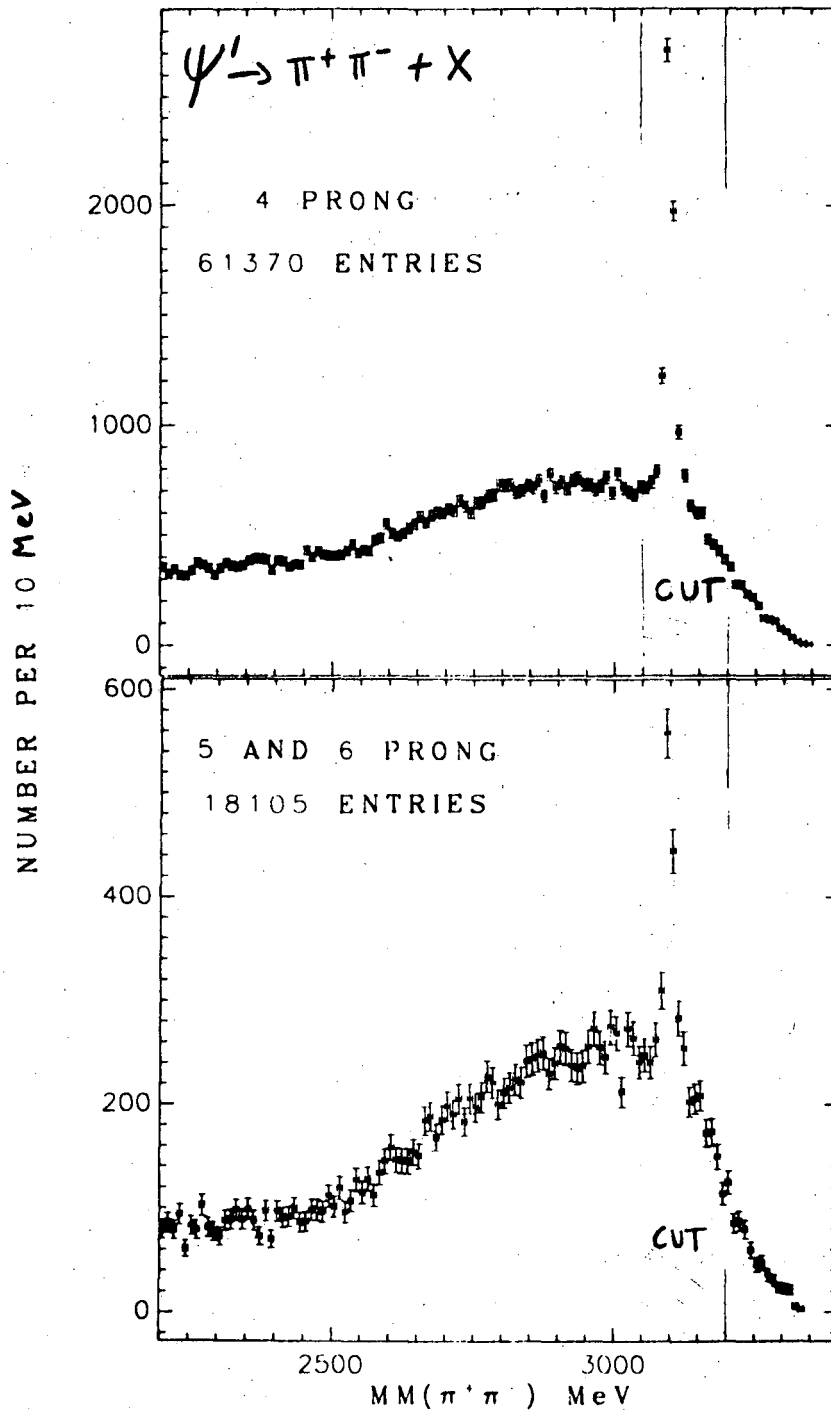
XBL 764-1617

Fig. 2. Missing mass distributions against $\pi^+\pi^-$ systems
in ψ' decay for four-prong and five- and six-prong events.
This data corresponds to a partial sample only and is
shown here to illustrate the "cascade cut."

"cascade cut." This involves cutting out those events for which a missing mass against the $\pi^+\pi^-$ system lies within the energy band 3.05 to 3.20 GeV. This cut is indicated in Fig. 2. For the four-prong events a further cut of $M(\pi^+\pi^-) >$ 2.8 GeV was made to exclude events of the type $\psi' \to \psi + \eta \to \mu^+\mu^-\pi^+\pi^-\pi^o$. In Fig. 3 is shown the resultant mass spectrum for channels (1), (2) and (3) respectively. All of these correspond to kinematically fitted data. Figures 4 and 5 show the data for the decay channels:

$$\psi' \to \gamma + (\pi^+\pi^- \text{ or } K^+K^-) \qquad\qquad (5)$$

and $\qquad\qquad \psi' \to \gamma + \pi^+\pi^- p\bar{p} \quad . \qquad\qquad\qquad (6)$

As may be noted from Fig. 3 there is good evidence in reactions (1) and (2) for three distinct X states, X(3415), X(3500), and X(3550). In addition we note a peak at (nearly) the full energy of the ψ'. This corresponds to the direct decay $\psi' \to 4\pi^\pm$, $\psi' \to 2\pi^\pm 2K^\pm$, etc. On careful inspection one can see that the mass lies $\sim$ 30 MeV below the ψ' mass. This arises because the fitting program for a 1C fit will still provide a "γ-ray" for these events and this introduces an artificial shift which is always downwards from the ψ' mass. In the unfitted data the events in these highest mass peaks do show the correct ψ' mass. Furthermore we can note that the direct decay into an even number of pions is G-parity suppressed and occurs only via an intermediate virtual photon. On the other hand $\psi' \to 2\pi^\pm 2K^\pm$ and $\psi' \to 2\pi^\pm p\bar{p}$ can proceed via the strong interactions and thus appear relatively enhanced when compared to the corresponding X decays.

In Fig. 6 is shown the angular distribution of the γ rays from channel (1) for the three X states. Figure 7a shows $M(\pi^+\pi^-)$ for reaction (1), while Fig. 7b shows $M(K^\pm\pi^\mp)$ for reaction (2). As may be noted, a strong ρ^o and $K^*(890)$ signal respectively is observed. The decay distributions for the other two X states are similar. Here it should also be noted that in Fig. 7a there are four $\pi^+\pi^-$ combinations per event, while in Fig. 7b there are only
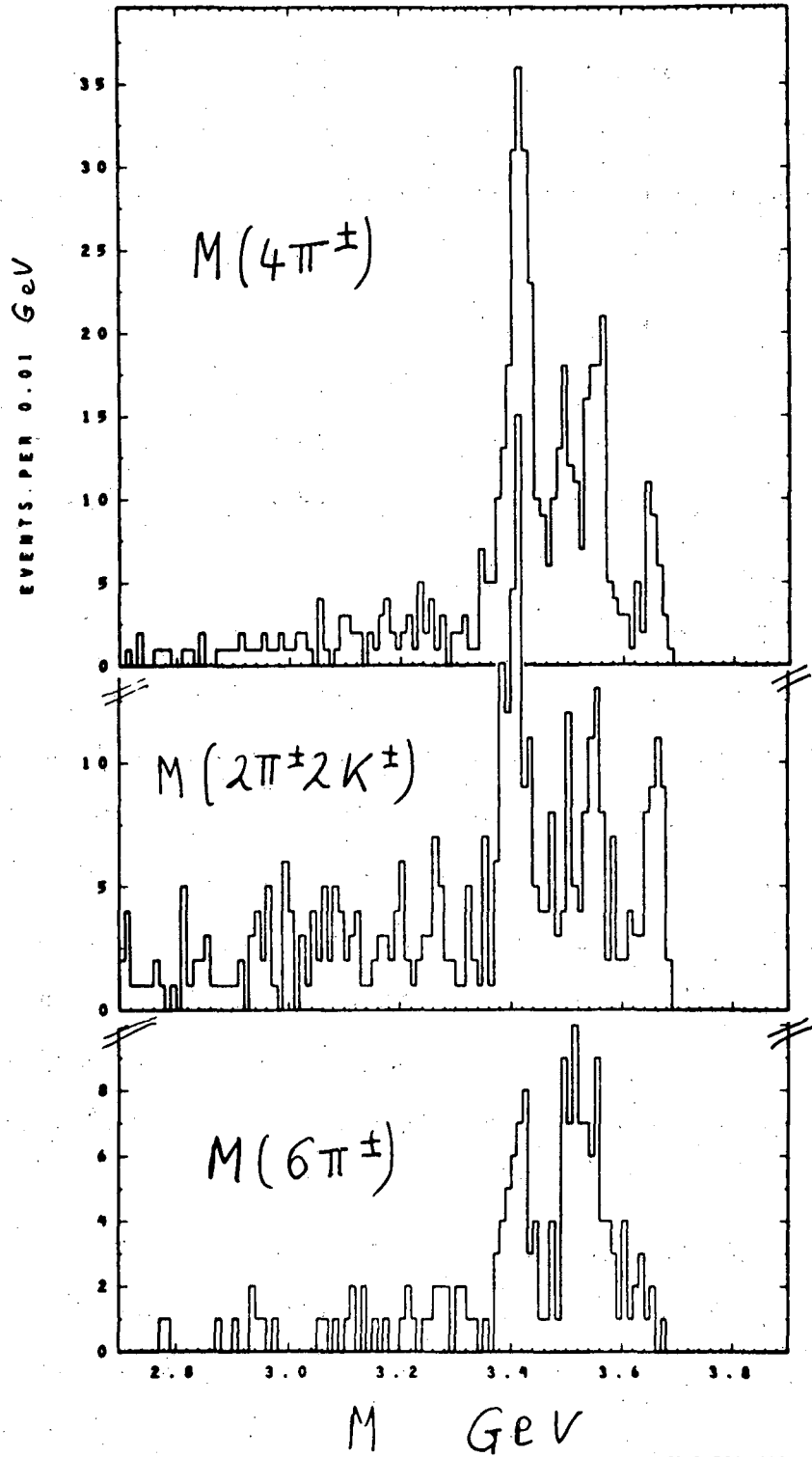
XBL 764-1618

Fig. 3. The kinematically fitted mass spectra for $4\pi^{\pm}$, $2\pi^{\pm}2K^{\pm}$ and $6\pi^{\pm}$ events from ψ' decay with cuts as discussed in the text.
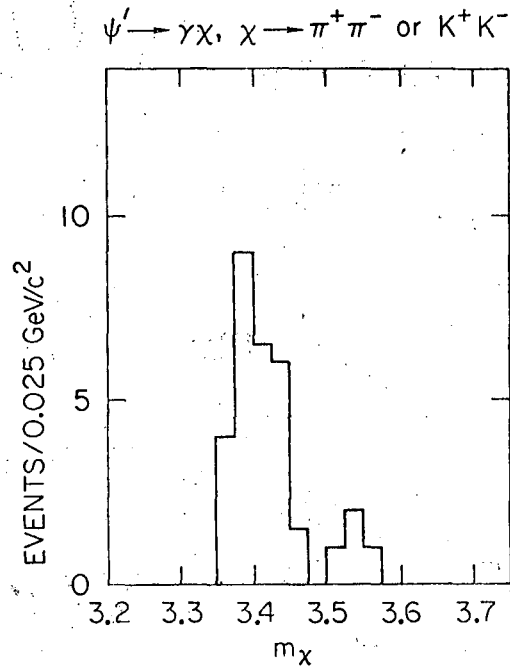
$$\psi' \rightarrow \gamma\chi, \ \chi \rightarrow \pi^+\pi^- \text{ or } K^+K^-$$

XBL 764-1620

Fig. 4. ψ' decay to $\pi^+\pi^-$ or K^+K^- with MM^2 consistent with missing γ, unfitted data.

$$\psi' \rightarrow p\bar{p}\pi^+\pi^- \ (+X_o) \qquad MM^2 < 0.03$$
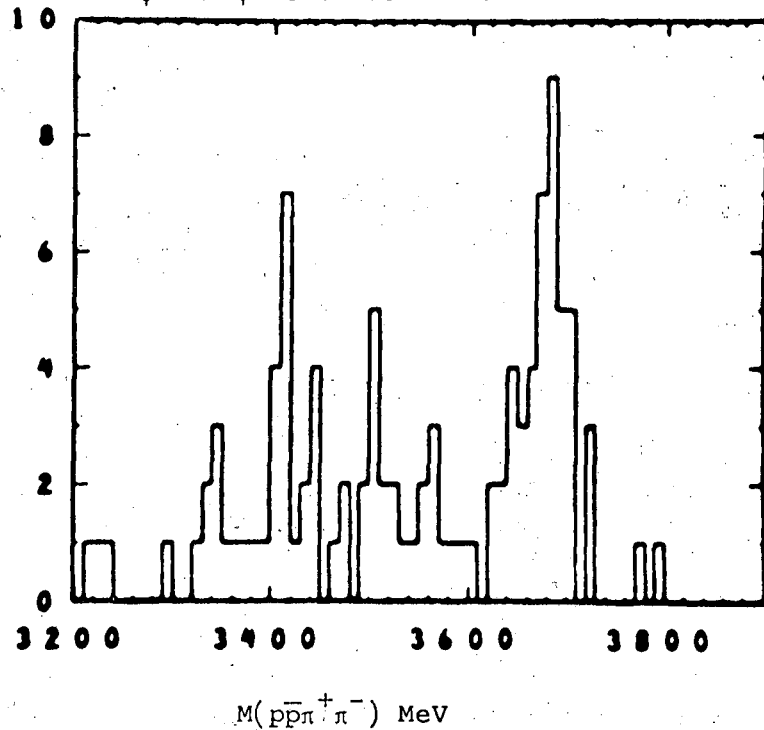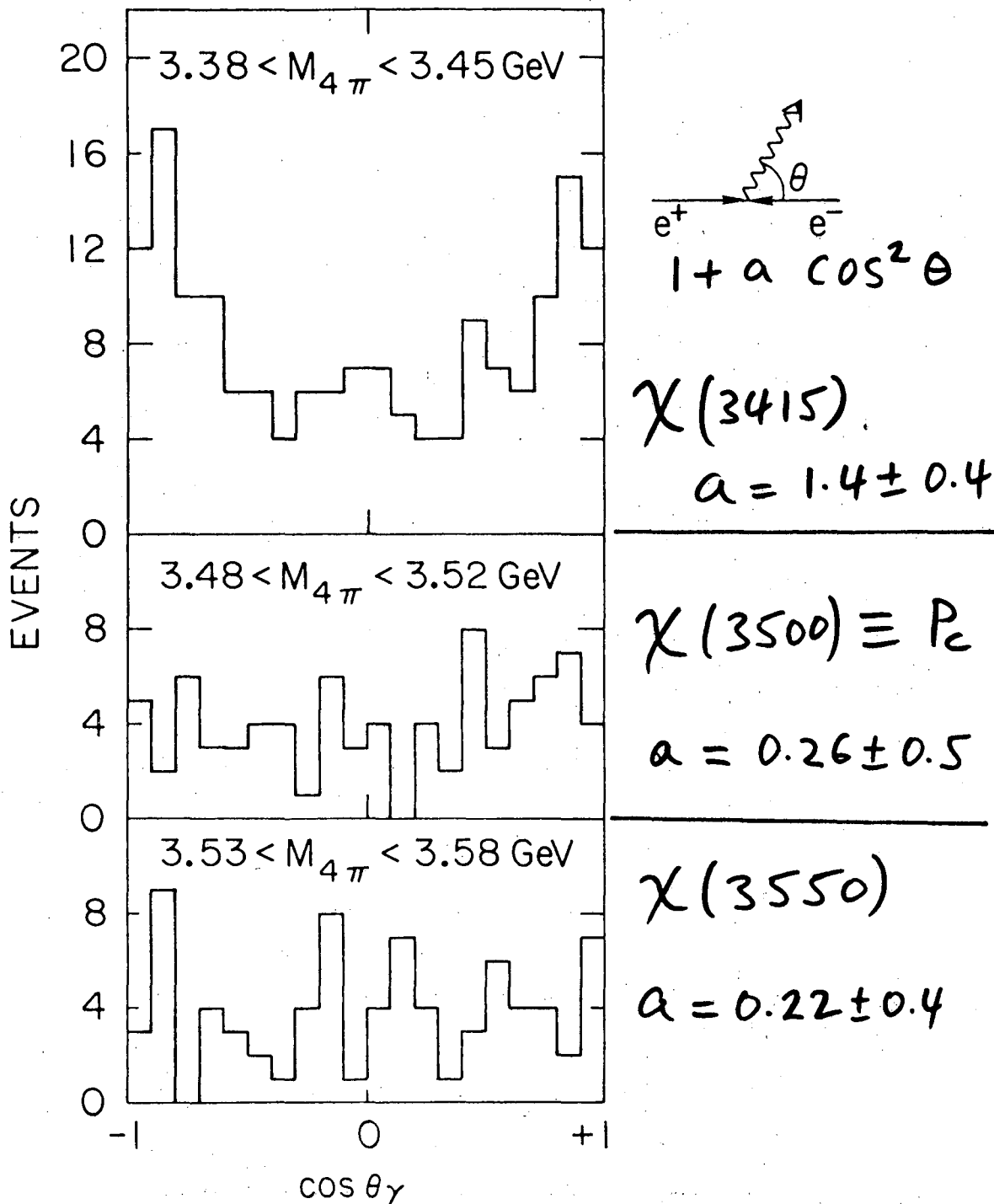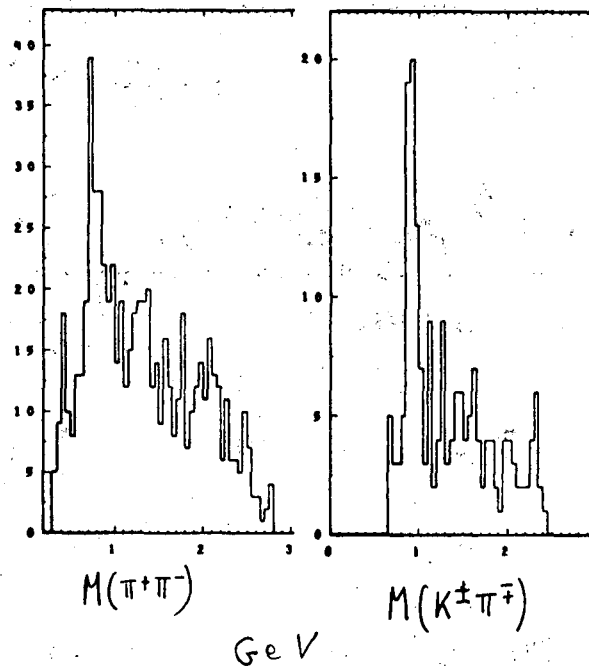
$\psi' \rightarrow \psi$ cascade cut out

$M(p\bar{p}\pi^+\pi^-)$ MeV

Fig. 5. ψ' decay to $\pi^+\pi^- p\bar{p}$ with cuts as discussed in text, unfitted data.

Fig. 6.   Angular distribution of the γ-rays for the three X states.

$$M(\pi^+\pi^-) \qquad M(K^{\pm}\pi^{\mp})$$

GeV

XBL 764-1619

Fig. 7. (a) $M(\pi^+\pi^-)$ for $X(3415) \to 4\pi^{\pm}$.
(b) $M(K^{\pm}\pi^{\mp})$ for $X(3415) \to 2\pi^{\pm}2K^{\pm}$.

two $K^{\pm}\pi^{\mp}$ combinations per event. From a triangle plot in two dimensions, there is no evidence for double ρ or double $K^*(890)$ production respectively.

1. Branching Fractions for the X States

We have preliminary results on the branching fractions B_f for the X states. Here B_f is composed of two components $B_f = B_\gamma B_h$ where B_γ is the branching ratio for $\psi' \to \gamma + X_i$ and B_h is the branching ratio for $X_i \to$ hadrons. The B_f values are given in Table I. These values are based on preliminary efficiency determinations and errors are estimated at $\pm 50\%$.

2. Quantum Numbers of the X States

From the fact the X states are produced by radiative decay of the ψ', $C = +1$ for all of them. If I-spin and G-parity are good quantum numbers for these states, from the fact that we observe a decay into even number of pions, $G = +$ for all of them, and from the relation $G = C(-1)^I$, we can infer that $I = 0$ for all of them. $I = 2$ is unlikely as it would involve

Table I. Preliminary values for branching fractions in ψ' decay. Uncertainties in these values are estimated at ± 50%.

$$B_f \times 10^3 \quad \pm 50\%$$

M_χ	$4\pi^\pm$	$2\pi^\pm 2K^\pm$	$6\pi^\pm$	$2\pi^\pm$ OR $2K^\pm$	$2\bar{\pi}^\pm$ $P\bar{P}$
3550	1.3	0.9			✓
			⎫ ✓		?
3500	1.0	0.6	⎭		
3415	3.0	2.0	1.3	1-2	0.5

$$B_f = B_\gamma B_h$$

$$B_\gamma : \quad \psi' \to \gamma + \chi$$

$$B_h : \quad \chi \to \text{Hadrons}$$

an unknown type of electromagnetic decay.

The γ-decay angular distribution shown in Fig. 6 can be expressed as:

$$1 + a \cos^2 \theta .$$

We then expect:

$$J = 0 \qquad a = 1$$

$$J = 1 \qquad a = -1/3 \left. \right\}$$ to lowest

$$J = 2 \qquad a = 0.06 \left. \right\}$$ multipole order

We note that the γ-decay distribution for X(3415) is consistent with J = 0; on the other hand we observe X(3415) → $\pi^+\pi^-$ or K^+K^- from Fig. 4. This implies J^P = 0^+, 2^+, etc. Combining this information we can conclude that for X(3415) J^{PC} = 0^{++}. We cannot at this time draw any conclusions on J^P assignments for the other X states.

B. The Inclusive γ-Ray Spectrum at the ψ and ψ'

We have studied the inclusive γ-ray spectrum from γ conversions in the 0.051 radiation length of material of the cylindrical scintillation counters, beam pipe, etc. Dalitz pairs (and internally converted γ-rays) also contribute to this sample. Figure 8 shows the γ-ray detection efficiency as a function of γ-ray energy. For $e^{\pm}$ momentum measurement the $e^{\pm}$ have to give at least one signal in the proportional chambers (R = 17, 22 cm) and one in each of the two innermost cylindrical spark chambers (R = 66, 91 cm). This implies a low momentum cutoff in perpendicular momentum ($P_{\perp}$) at ~ 50 MeV/c for each $e^{\pm}$ track. For definiteness in Monte-Carlo efficiency calculations we apply a safe cutoff at $P_{\perp}$ = 55 MeV/c in the software. As a consequence of this cutoff our efficiency for γ detection drops rapidly below 200 MeV γ-rays.
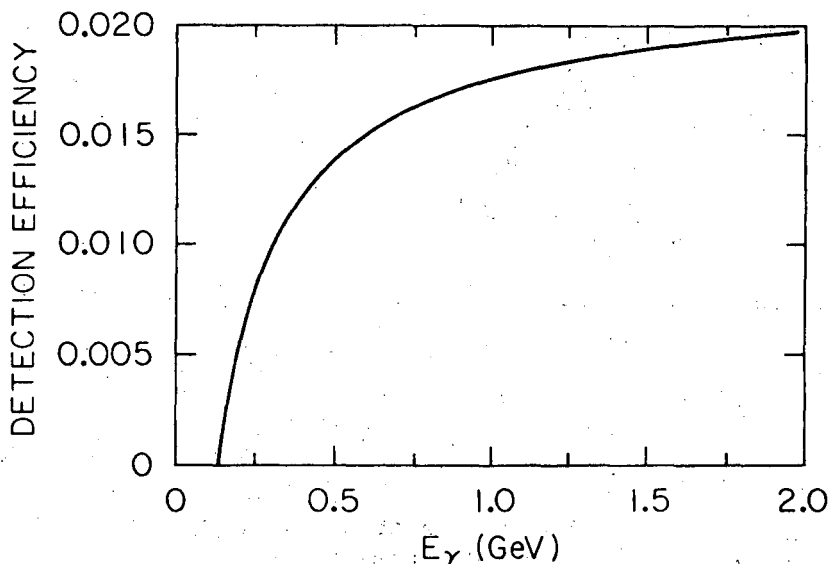
XBL 764-1621

Fig. 8. SPEAR detector as γ spectrometer. Detection efficiency.
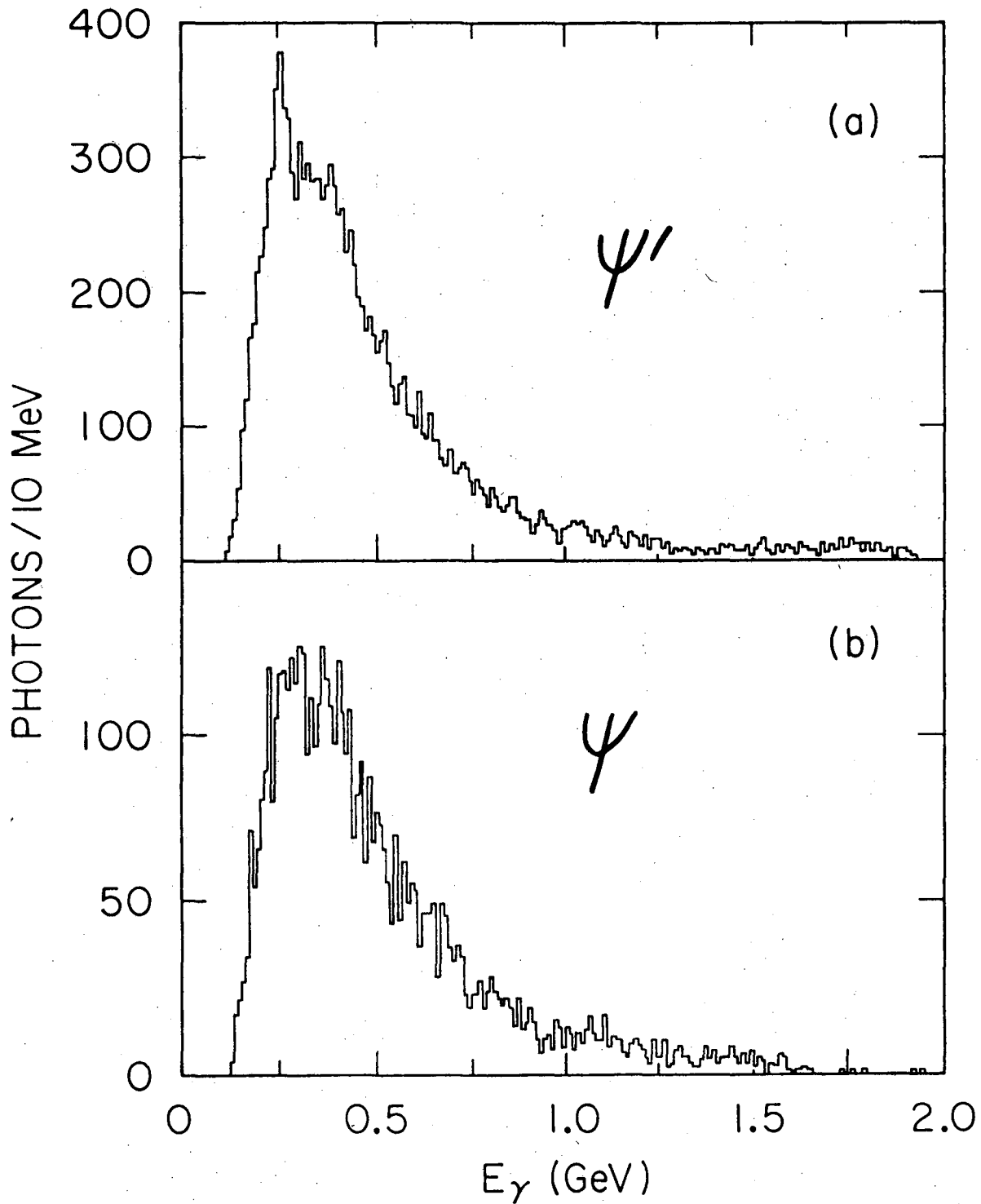
Fig. 9. γ-ray spectrum at ψ' and ψ as obtained from γ conversion in the cylindrical counters surrounding the beam pipe.

XBL 764-1616

The measured γ-ray spectrum for ψ and ψ' decay is shown in Fig. 9. We note a clear signal in the ψ' decay spectrum at $E_\gamma = 263 \pm 10$. This gives a mass for the corresponding X states of ~ 3410 MeV. The branching ratio $B_{\psi'\gamma'}$ estimated for a γ decay angular distribution of $1 + \cos^2 \theta$, is $8.5 \pm 4\%$.

C. The Reaction $\psi' \to \gamma\gamma\psi$

By demanding a converted γ-ray together with final state ψ decay

$$\psi \to \mu^+\mu^- \tag{7}$$

$$\text{or} \qquad \psi \to e^+e^- \tag{8}$$

we have studied the reaction:

$$\psi' \to \gamma\gamma\psi \ . \tag{9}$$

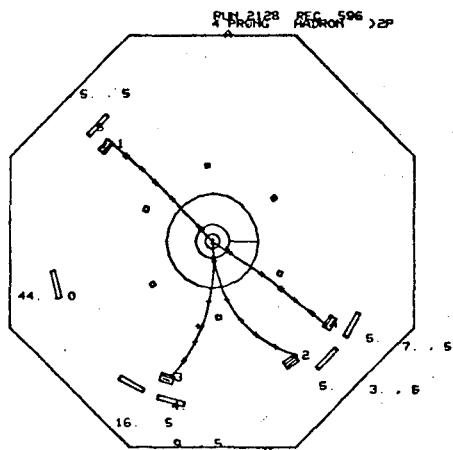An example of this reaction with the ψ decay mode (7) is shown in Fig. 10.

XBL 764-1624

Fig. 10. Computer reconstruction of an example of the reaction

$$\psi' \to \gamma + P_c$$
$$ \downarrow \to \gamma + \psi$$
$$ \downarrow \qquad \downarrow \to \mu^+\mu^-$$
$$ \downarrow \to e^+e^-$$
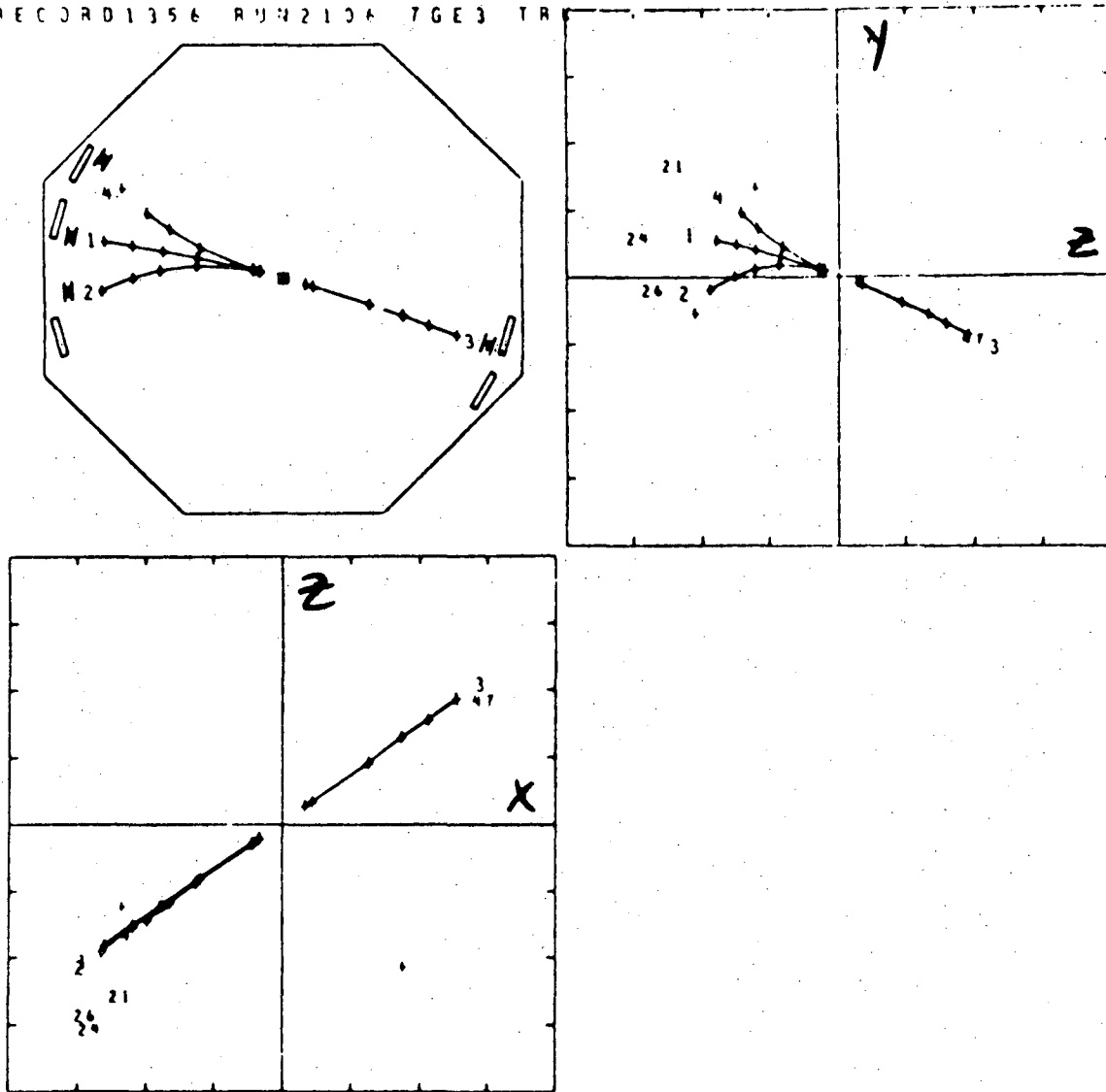$$ \text{conv.}$$

▭ trigger counters latched;

▭ shower counters latched.

Note that the first γ-ray converts in a shower counter.

In using the events with $\psi \to e^+e^-$ care must be taken to eliminate a background due to final state radiation in the decay $\psi' \to e^+e^-$. An example of this process is shown in Fig. 11. After elimination of events consistent with π^0 or η^0 production we remain with a sample of 21 events corresponding to reaction (9). There still remains the ambiguity as to which γ-ray comes from ψ' decay and which from the decay of possible intermediate states. We thus compute two solutions for each event: the "low mass $(\psi\gamma)$" and "high mass $(\psi\gamma)$" solutions.

Fig. 11. Computer reconstruction of an example of

$$\psi' \rightarrow e^+e^- + \gamma$$

$$\underset{\text{conv.}}{\mathop{|}\limits_{\rightarrow}} e^+e^-$$

These are given in a scatter plot in Fig. 12. As may be noted the events

cluster in three regions and furthermore the projections on the "high mass

solution" give three narrow peaks, while the other projection gives a broad

distribution. This suggests that we are observing three narrow states at

masses 3545, 3505, and 3415 MeV. In the projection on the y axis one is then

presumably combining the ψ and a Doppler-shifted γ, emitted from the decay of

a recoiling intermediate state. The expected Doppler broadening is ~ 50 MeV

and is consistent with the observation. Table II gives the branching fractions

where the errors are dominated by the statistical error of a small number of

events.

Table II. Preliminary values for branching fractions
of $\psi' \rightarrow \gamma\gamma\psi$ with conversion of one γ-ray.
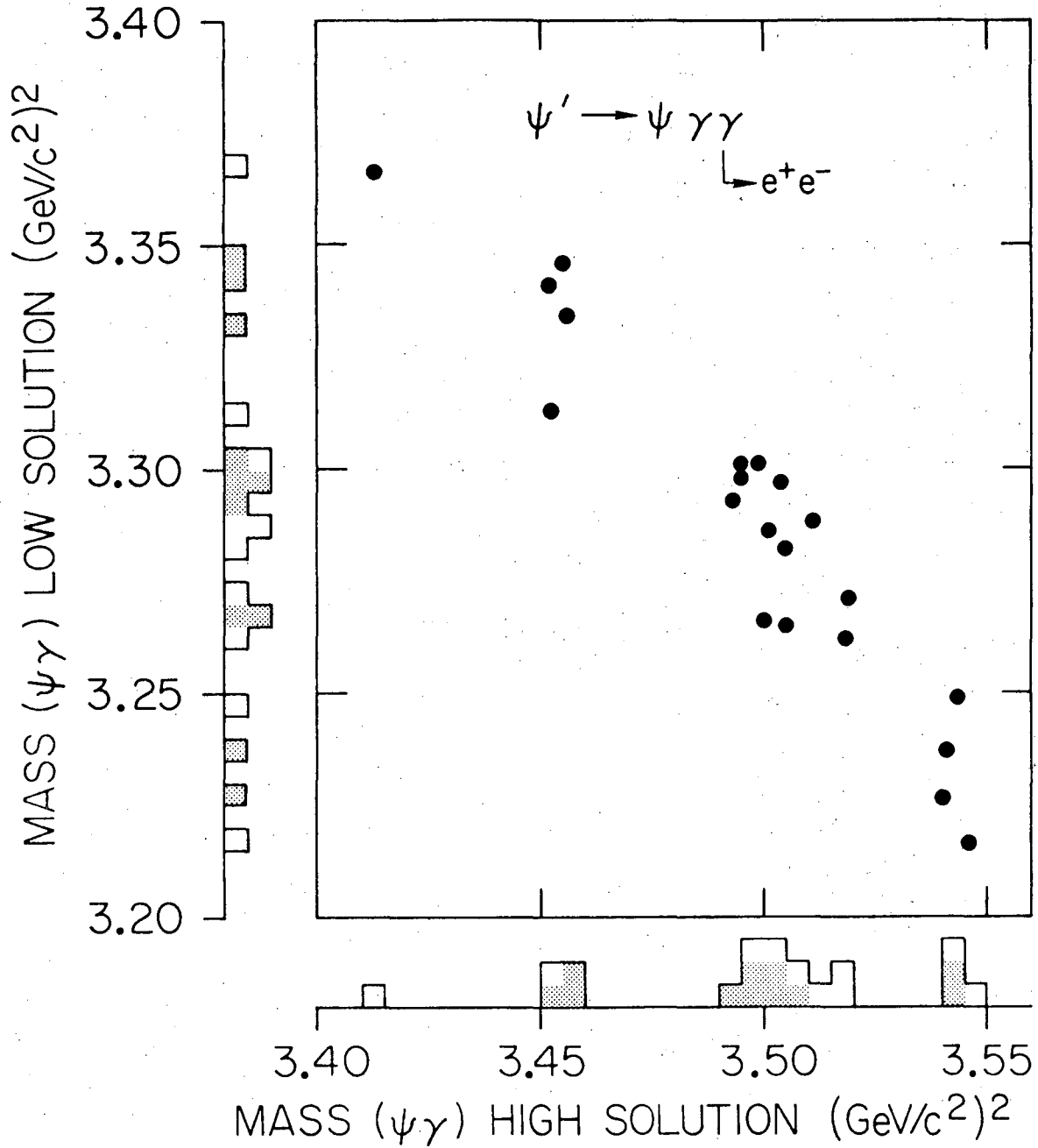
$$\psi' \rightarrow \gamma\gamma\psi$$
$$\hookrightarrow e^+e^-$$

$$B_f = B_{\gamma\psi} \cdot B_{\gamma\chi}$$

MeV	EVENTS	Bf	$B_{\gamma\psi'}$
3545	4	1%	
3505	12	3%	
3455	4	1%	
3415	1	0.25%	8.5±4%

RESOLUTION ~ 8MeV

Fig. 12. Scatter plot of the $\psi\gamma$ mass; "low mass ($\psi\gamma$)" vs "high mass ($\psi\gamma$)" solutions.

D.   <u>Search for the η_c With $p\bar{p}$ Decay Mode</u>

We do not observe any mass peak which could correspond to

$$\psi \rightarrow \gamma + X \tag{10}$$
$$|_{\rightarrow\ p\bar{p}}\ .$$

Figure 13 shows a scatter plot of β vs p for two-prong events at the ψ.   The

data was preselected so that each event had at least one prong with mass meas-

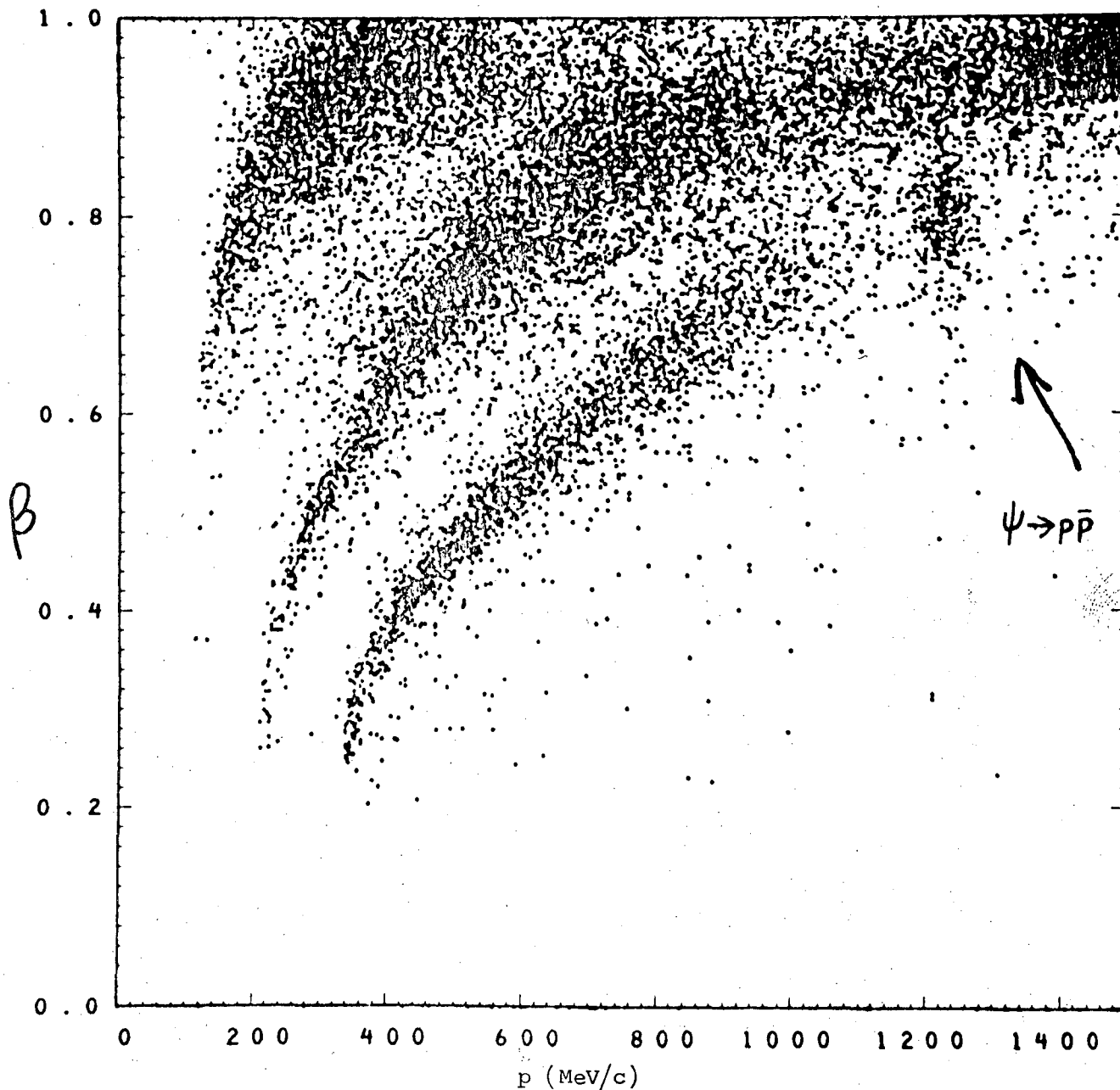ured from time of flight > 350 MeV.   Thus the separation between the pion

Fig. 13.   Scatter plot of β from time of flight versus momentum.

band and K band is in part artificial. However the separation between kaons

and protons is real. Figure 14 shows a plot of p_p vs $p_{\bar{p}}$ for two-prong events.

Figure 15 shows a plot of normalized missing momentum p/E_o vs normalized mass

of the $p\bar{p}$ system $M(p\bar{p})/(2E_o)$. The relevant features are marked on the plot.

Parenthetically we note a large signal corresponding to

$$\psi \rightarrow p\bar{p}\eta \qquad\qquad B = (1.9 \pm 0.35) \times 10^{-3} \quad . \qquad\qquad (11)$$

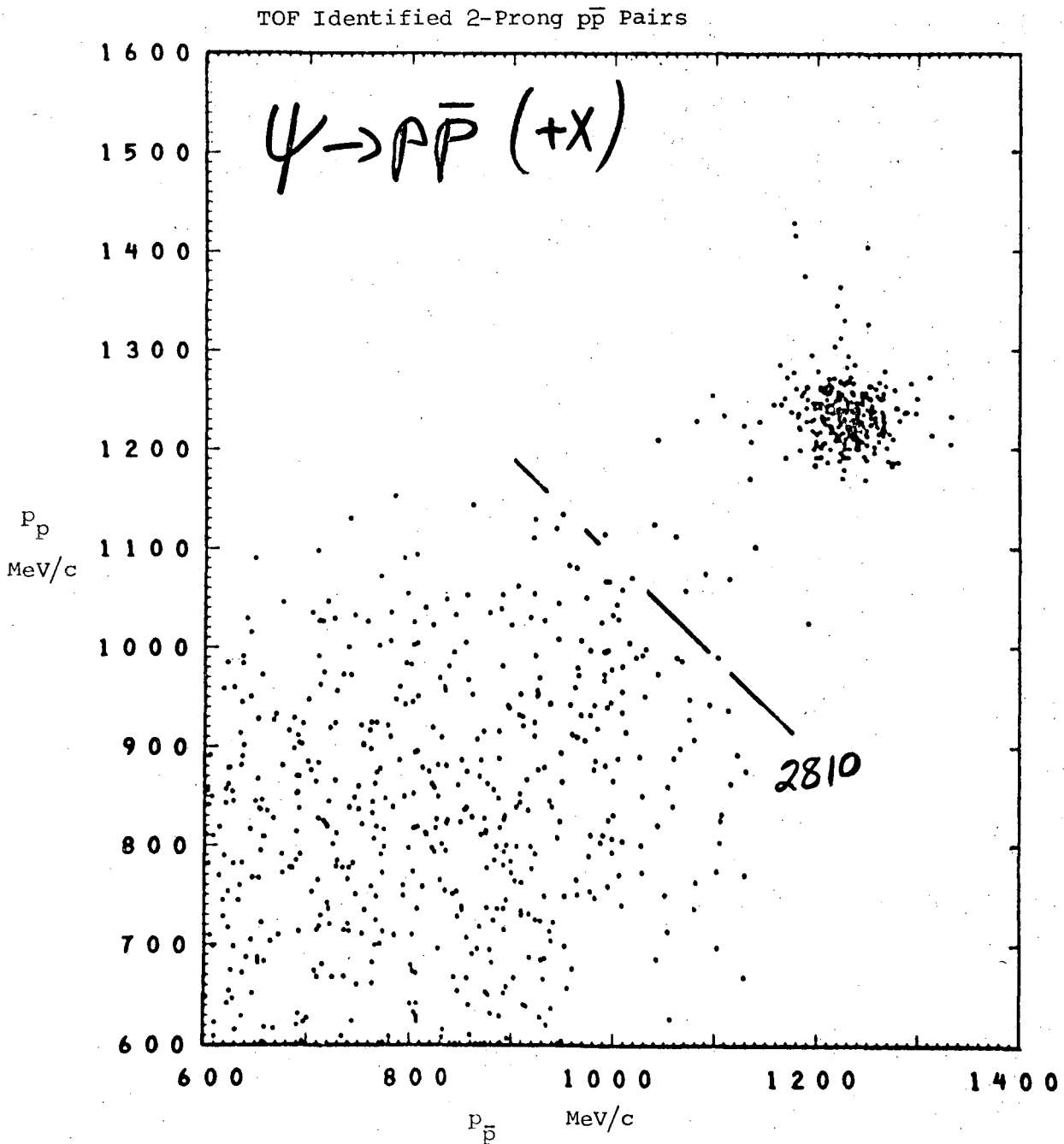TOF Identified 2-Prong $p\bar{p}$ Pairs

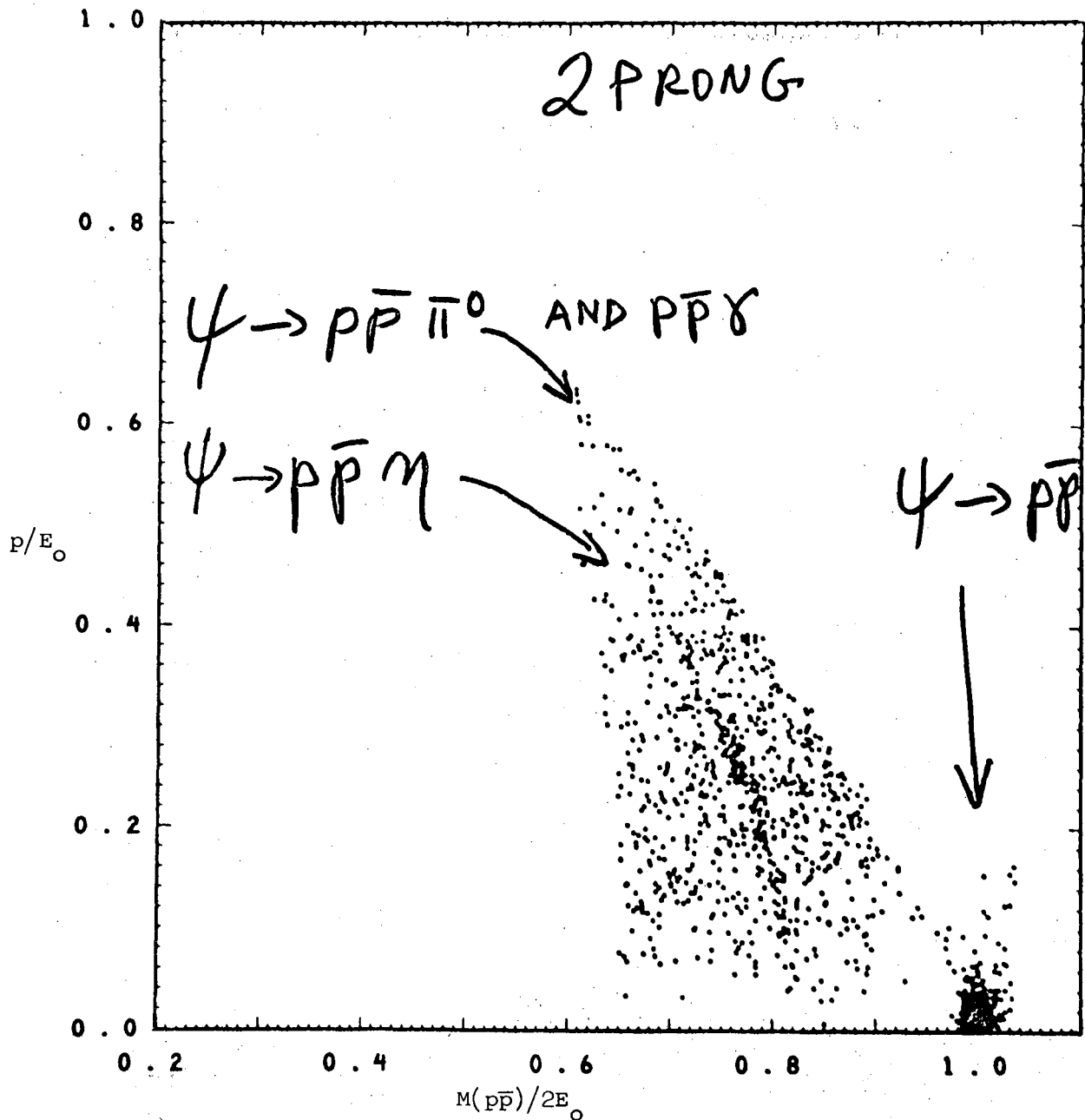Fig. 14. Scatter plot of proton momentum versus antiproton momentum.

Fig. 15. Scatter plot of normalized momentum vs normalized mass of the $p\bar{p}$ system.

In Figs. 13, 14 and 15 we note the cluster corresponding to

$$\psi \rightarrow p\bar{p} \qquad B = (2.0 \pm 0.15) \times 10^{-3}, \sim 300 \text{ events}. \qquad (12)$$

The line sketched in Fig. 14 corresponds to the 2810 MeV mass region. As may

be noted for both Figs. 14 and 16 which is the $M(p\bar{p})$ mass projection for low

MM ($MM^2 < 0.03$ GeV), we see no mass peak near 2800 MeV. The upper limits

corresponding to this data are given in Table III.

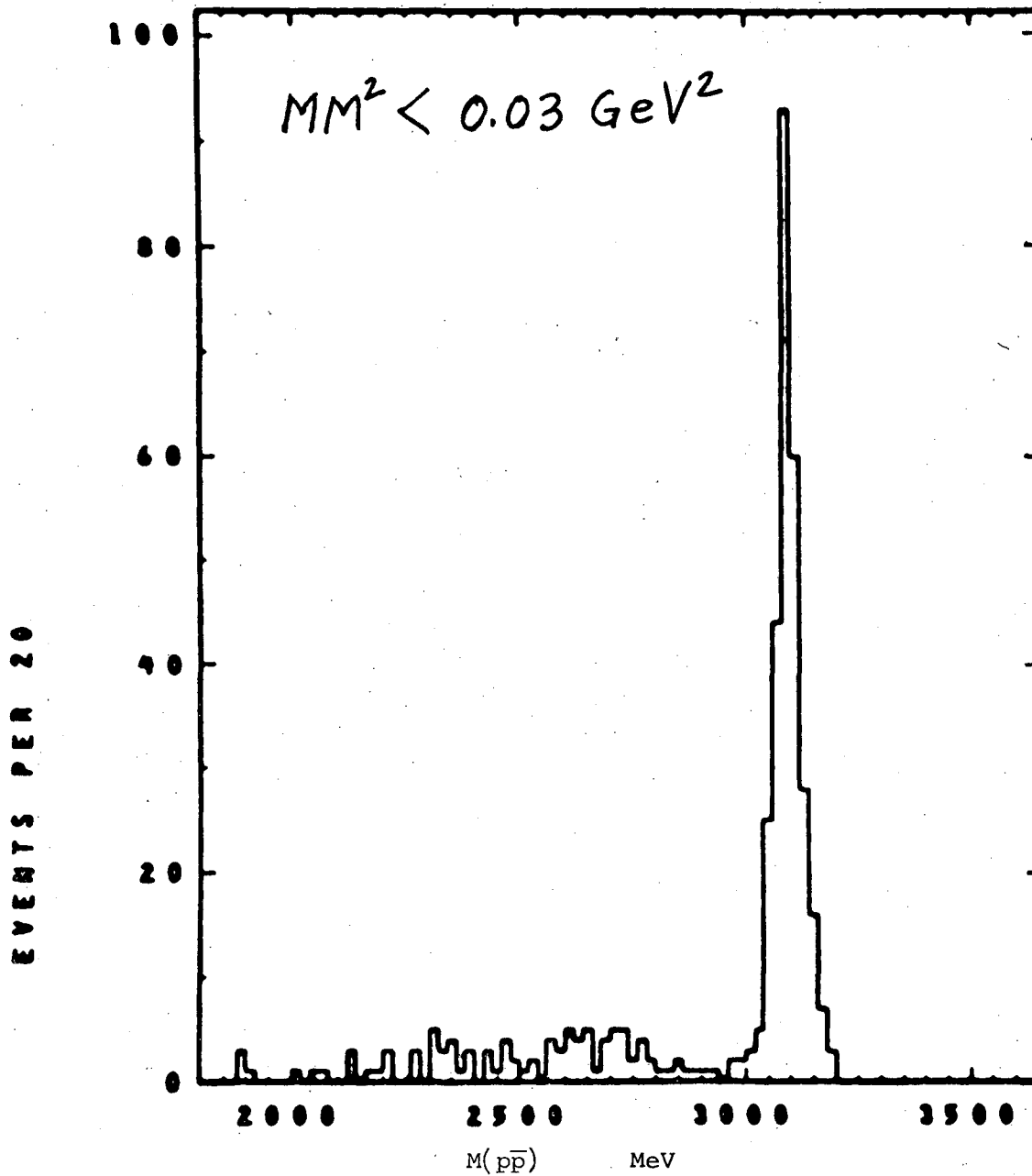Fig. 16. Mass of the p$\bar{\text{p}}$ system for missing mass cut MM^2 < 0.03 Gev^2.

The results presented here are the work of the LBL-SLAC Collaboration at

SPEAR, whose members are: G. S. Abrams, S. Alam, A. M. Boyarski, M. Breidenbach,

F. Bulos, W. Chinowsky, R. G. DeVoe, G. J. Feldman, G. E. Fischer, C. E.

Friedberg, D. Fryberger, G. Goldhaber, G. Hanson, D. Hartill, B. Jean-Marie,

A. D. Johnson, J. A. Kadyk, R. R. Larsen, A. Litke, D. Lüke, V. Lüth, H. L.

Lynch, R. Madaras, C. C. Morehouse, H. K. Nguyen, J. M. Paterson, M. L. Perl,

Table III. Upper limits in the branching ratio B for the reaction

$$\psi \to \gamma + X$$
$$ {\large\llcorner}\to p\bar{p} \; .$$

Energy of peak (GeV)	90% C.L. Upper limit Number of events	B
2.85 ± 0.05	4.0	$< 3 \times 10^{-5}$
2.80 ± 0.05	5.8	$< 4 \times 10^{-5}$
2.70 ± 0.05	12.0	$< 8 \times 10^{-5}$
2.65 ± 0.05	13.6	$< 9 \times 10^{-5}$

I. Peruzzi, M. Piccolo, F. M. Pierre, P. Rapidis, B. Richter, B. Sadoulet,

R. F. Schwitters, J. Siegrist, W. Tanenbaum, G. H. Trilling, F. Vannucci,

J. S. Whitaker, F. C. Winkelmann, and J. E. Wiss.

FOOTNOTES AND REFERENCES

1. Our earlier trigger requirements consisted of a coincidence between the
central cylindrical counters surrounding the beam pipe and two (or more)
of the trigger counters at radius 1.5 meters, where at least two have an
associated shower counter. The entire system was gated to the e^+e^-
collision time. Here an associated shower counter means a shower counter
located within the immediate vicinity of the latched trigger counter.
This trigger thus requires at least two charged particles to reach the
shower counters. The new "relaxed" trigger requires a coincidence between
the central cylindrical counters and any two (or more) of the trigger
counters where at least one of these occurs with an associated shower
counter; in addition, at least one signal in the proportional chambers
was required. Thus the new trigger requires one particle to penetrate to
the shower counters but the second particle need only reach the trigger
counters.

2. G. J. Feldman, B. Jean-Marie, B. Sadoulet, F. Vannucci et al., Phys. Rev.

Letters 35, 821 (1975).

3. G. H. Trilling, A. D. Johnson et al., in preparation.

4. J. S. Whitaker, W. Tanenbaum et al., in preparation.

5. W. Tanenbaum, J. S. Whitaker et al., Phys. Rev. Letters 35, 1323 (1975).

6. W. Braunschweig et al., Physics Letters 57B, 407 (1975).

7. M. Piccolo, I. Peruzzi et al, in preparation.